EUROPEAN JOURNAL OF CANCER 45 (2009) 1518–1526

available at www.sciencedirect.com

ScienceDirect

journal homepage: www.ejconline.com

A systems pathology model for predicting overall survival in patients with refractory, advanced non-small-cell lung cancer treated with gefitinib

Michael J. Donovan[a,*], *Angeliki Kotsianti*[a], *Valentina Bayer-Zubek*[a], *David Verbel*[a], *Mikhail Teverovskiy*[a], *Carlos Cordon-Cardo*[a,b], *Jose Costa*[a,c], *F. Anthony Greco*[d], *John D. Hainsworth*[d], *Dinah V. Parums*[e]

[a]*Aureon Laboratories, 28 Wells Avenue, Yonkers, NY 10701, United States*
[b]*Columbia University, NY, United States*
[c]*Yale University School of Medicine, New Haven, CT, United States*
[d]*Sarah Cannon Cancer Center, Nashville, TN, United States*
[e]*AstraZeneca, Alderley Park, UK*

ARTICLE INFO

Article history:
Received 9 December 2008
Received in revised form 28 January 2009
Accepted 2 February 2009
Available online 9 March 2009

Keywords:
Non-small-cell lung carcinoma
Statistical models
Epidermal growth factor receptor
Gefitinib
Clinical pathology
Survival analysis
Biological tumour markers

ABSTRACT

Purpose: To identify clinical and biometric features associated with overall survival of patients with advanced refractory non-small-cell lung cancer (NSCLC) treated with gefitinib.

Experimental design: One hundred and nine diagnostic NSCLC samples were analysed for EGFR mutation status, EGFR immunohistochemistry, histologic morphometry and quantitative immunofluorescence of 15 markers. Support vector regression modelling using the concordance index was employed to predict overall survival.

Results: Tumours from 4 of 87 patients (5%) contained EGFR tyrosine kinase domain mutations. A multivariate model identified ECOG performance status, and tumour morphometry, along with cyclin D1, caspase-3 activated, and phosphorylated KDR to be associated with overall survival, concordance index of 0.74 (hazard ratio (HR) 5.26, *p*-value 0.0002).

Conclusions: System-based models can be used to identify a set of baseline features that are associated with reduced overall survival in patients with NSCLC treated with gefitinib. This is a preliminary study, and further analyses are required to validate the model in a randomised, controlled treatment setting.

1. Introduction

The over-expression of epidermal growth factor receptor (EGFR) in a variety of solid tumours, including non-small-cell lung cancer (NSCLC), has made it an attractive target for selective molecular therapeutics, specifically for tyrosine kinase inhibitors (TKIs) such as gefitinib (IRESSA). Although initial results for gefitinib in pretreated patients were promising, in two pivotal Phase III trials patients treated with gefitinib did not demonstrate significantly better overall or progression-free survival compared with the placebo group.[1,2] Furthermore, in the Phase III, placebo-controlled IRESSA Survival Evaluation in Lung Cancer (ISEL) trial, gefitinib monotherapy was associated with some improvement in

* *Corresponding author:* Tel.: +1 914 377 4037; fax: +1 914 377 4001.
E-mail address: Michael.Donovan@AUREON.com (M.J. Donovan).
0959-8049/$ - see front matter
doi:10.1016/j.ejca.2009.02.004

overall survival; however, the results did not reach statistical significance.[3]

An objective response to gefitinib has been linked to several molecular, demographic and clinical-pathologic factors including activating mutations in the ATP pocket of EGFR, tumour histology (adenocarcinoma – bronchoalveolar variant), amplification of the EGFR gene, Asian race, female gender, non-smoking history and good performance status.[4–7] Encouraging data from the recent iTARGET trial demonstrated an improved outcome when patients were treated with first-line gefitinib therapy based on their EGFR mutation status.[8] Although the results need to be compared with more traditional therapies, the study does provide some preliminary evidence for the future of 'genotype-based' treatment decision-making. In addition, evidence from the ISEL trial suggested that high EGFR gene copy number was predictive of clinical benefit and survival. Of note, a recent open-label Phase III study compares gefitinib with docetaxel in patients with locally advanced disease; however, this did not find an association with EGFR gene copy number and outcome.[9] Both the studies illustrate the importance of deriving base line characteristics from the patient's primary tumour sample when developing a comprehensive management and treatment plan, and indicate that different patients derive different degrees of clinical benefit from treatment with EGFR TKIs.

We previously developed models to predict disease progression and therapeutic outcome for patients with prostate and breast cancers using a systems pathology platform.[10–13] In this approach, conventional clinical-pathologic information is integrated with biometric features from the tumour specimen, using machine learning to interpret the complex data sets.[10,12] In the current study, we analysed 109 patients with refractory NSCLC, all treated with gefitinib using an Expanded Access Programme (EAP). We sought to determine EGFR mutation status in the patients' diagnostic tumour and to use systems pathology to identify a baseline phenotype predictive of overall survival.

2. Methods

2.1. Patients and tissues

This study was approved by the institutional review board of the Sarah Canon Cancer Research Centre, and where appropriate all patients provided informed consent. The initial cohort consisted of 284 US patients with advanced refractory NSCLC treated with 250 mg gefitinib orally each day. Six clinical variables were analysed: gender, smoking history, age at diagnosis, tumour histology, number of prior chemotherapies and ECOG performance status (a scale ranging from 0, healthy, to 5, death from disease). Unstained de-paraffinised slides (fine needle aspirates, cell pellets or cytospins) and/or paraffin blocks from the diagnostic specimen were evaluated with hematoxylin and eosin (H&E) for tumour content. All biomarkers were analysed without knowledge of clinical outcome.

2.2. EGFR mutation analysis

Two sequential 20-μm sections from each paraffin block or ⩾8 unstained sections from paraffin slides were analysed. Genomic DNA was obtained from de-paraffinised samples by incubation with proteinase K, then by chloroform extraction and ethanol precipitation. EGFR mutations were analysed primarily by DNA sequencing of exons 19, 20 and 21, and secondarily using the amplification refractory mutation system (ARMS), specifically allele-specific polymerase chain reaction (PCR) to detect the L858R mutation and del G2235-A2249. Patients were considered mutation positive if a mutation in the tyrosine kinase domain was detected by either ARMS or sequencing in both forward and reverse directions in at least two independent PCR products.

2.3. Histologic morphometry

H&E-stained slides were prepared from the original blocks or unstained sections. One to six images from representative areas of tumour were acquired with an Olympus bright-field microscope at 20× magnification using a SPOT Insight QE camera (KAI2000). Image analysis software[10] classified image objects as histopathological cellular elements, exhibiting particular colour channel values, generic shape features (e.g. area and length), and spatial relationship properties (e.g. amounts of lumen relative to total tissue), from which statistics were generated. Due to differences in sample preparation (i.e. cytospin, needle biopsy and tissue resection) fixation, staining, and tissue quality, several different scripts were developed for image segmentation.

2.4. EGFR immunohistochemistry

EGFR was analysed by immunohistochemistry using the EGFR pharmDX kit (DAKO, Glostrup, Denmark). A staining index with range 0–300 was calculated for each sample by multiplying each intensity level (0–3) by the percentage of cells at that intensity level.

2.5. Multiplex (M-Plex™) biomarker assessment

Fifteen antibodies were selected (Table 1). Each antibody was initially evaluated by immunohistochemistry on a series of cell lines and/or control lung cancer tissue samples with appropriate negative controls. To confirm specificity of the pEGFR and pERK antibodies, extracts of A431 NSCLC cells with or without EGF treatment were immunoprecipitated with these antibodies, followed by Western blotting. Similar tests were performed with pKDR in HUVEC cell lines activated with VEGF. In addition, for both EGF and VEGF, treated and non-treated cells were processed for routine immunohistochemistry. The 15 antibodies were organised into six multiplex formats (Table 1).

After de-paraffinisation and rehydration of tissue samples, slides were boiled in a microwave oven for 7.5 min in 1X Reveal Solution (BioCare Medical, Concord, CA) for antigen retrieval. After cooling for 20 min at room temperature, slides were washed twice for 3 min in phosphate-buffered saline (PBS).

To help permeate the cellular structures, samples were incubated in PBT (PBS with 0.2% Triton X-100) at room temperature for 30 min, followed by three rinses of 3 min each in PBS. To reduce autofluorescence, samples were incubated

Table 1 – Antibodies and multiplex immunofluorescence groupings.

M-plex group	Antibody	Vendor	Catalog #	Isotype	Dilution	Fluorescent label
1	Cytokeratin 18	Vector	VC-C414	Mouse IgG1	1:250	1° – 488
	Cyclin D1	BioCare Med.	CP236B	Rabbit IgG	1:100	1° – 568
2	Cytokeratin 18	Vector	VC-C414	Mouse IgG1	1:250	1° – 488
	Ki-67	Ventana	790-2910	Mouse IgG1	1:75 of pre-diluted	2° – 555
	PI3 kinase	Cell Signalling	3821	Rabbit IgG	1:20	1° – 568
	Caspase-3 activated	Chemicon	ab3623	Rabbit IgG	1:5	2° – 594
3	Cytokeratin 18	Vector	VC-C414	Mouse IgG1	1:200	1° – 488
	CD-34	Dako	M7165	Mouse IgG1	1:50	2° – 555
	p-mTOR	Cell Signalling	ab2971	Rabbit IgG	1:50	1° – 568
	pERK	Cell Signalling	ab4376	Rabbit IgG	1:5	2° – 594
4	Cytokeratin 18	Vector	VC-C414	Mouse IgG1	1:200	1° – 488
	pAKT S473	Abcam	ab4802	Rabbit IgG	1:20	1° - 555
	PTEN	NeoMarkers	MS1797	Mouse IgG1	1:50	2° – 568
	KDR [VEGFR2]	Upstate	07-158	Rabbit IgG	1:450	2° – 594
5	Cytokeratin 18	Vector	VC-C414	Mouse IgG1	1:250	1° – 488
	VEGF	Abcam	ab1316	Mouse IgG1	1:50	2° – 555
	pKDR	Upstate	07-374	Rabbit IgG	1:150	2° – 594
6	Cytokeratin 18	Vector	VC-C414	Mouse IgG1	1:10	2° – 488
	EGFR	Dako	K1492	Mouse IgG1	Pre-diluted	1° – 555
	pEGFR, Y1068	Abcam	ab5644	Rabbit IgG	1:250	1° – 594

in acid alcohol (1% HCl in 70% ethanol) at room temperature for 20 min, followed by three rinses of 3 min each in PBS. Slides were blocked in IF Blocking Reagent (0.5 mg/ml bovine serum albumin in PBS) at room temperature for 20 min. Slides were then advanced to hybridisation without additional washes.

A cocktail of one mouse IgG1 antibody and one rabbit IgG antibody was made using previously determined titres (Table 1) in IF Blocking Reagent. This cocktail (100 μl) was applied to the tissue sample. Samples were incubated in a humidity chamber at room temperature for 1 h, then rinsed for 5 min each in PBT, then twice for 3 min each in PBS.

For labelling, a cocktail of the appropriate Zenon Alexa Fluor Rabbit IgG label and Mouse IgG1 label (Invitrogen, Carlsbad, CA) for the primary antibodies was made in IF Blocking Reagent at 1:50 dilution for each Fab fragment. This labelling cocktail (100 μl) was applied to the tissue samples. Samples were incubated in a humidity chamber at room temperature for 30 min, then rinsed twice. The hybridisation and labelling steps were repeated for each subsequent group of antibodies included in the multiplex. Up to two more rounds of antibody hybridisation and labelling were possible.

Samples were fixed by incubation in 10% formalin at room temperature for 10 min, then rinsed twice for 3 min each in PBS. Approximately 25.0 μl of *SlowFade* Gold antifade reagent (Invitrogen) with DAPI mounting solution was applied to the samples, which were then cover slipped. Samples were stored at –20 °C until the time of analysis.

Fluorescence images were acquired using a CRI Nuance multispectral camera (Cambridge Research and Instrumentation, Woburn, MA) mounted on a Nikon 90i automated fluorescence microscope, and were controlled by MetaMorph software. Images were saved as quantitative greyscale TIFF images (1280 by 1024 pixels). For the selected regions of interest, DAPI was recorded at 480 nm using a bandpass DAPI filter (Chroma, Rockingham, VT). Alexa 488 was captured between 520 and 560 nm in 10-nm intervals using an FITC filter (Chroma). Custom-made longpass filters (Chroma) were used to record Alexa 647 between 640 and 720 nm in 10-nm intervals and to record Alexa 555, 568 and 594 between 570 and 670 nm in 10-nm intervals. Representative regions for each dye were allocated to create a spectral library for the spectral un-mixing process.

2.6. *Generation of immunofluorescent features*

Immunofluorescent scripts for each antibody:antigen pair were developed using control lung cancer tissue samples. The scripts were designed based on the expected cellular distribution of each protein (nuclear for cyclin D1, Ki67, PTEN and phosphorylated ERK [pERK]; cytoplasmic for CK18, caspase-3a and VEGF; nuclear/cytoplasmic for phosphorylated AKT; membrane for EGFR and KDR; and cytoplasmic/membrane for phosphorylated KDR [pKDR], phosphorylated mTOR, PI3K and phosphorylated EGFR [pEGFR]). The scripts utilise the greyscale image to identify area and subsequent fluorescent intensity for each marker. The image analysis scripts overlay morphologic attributes (i.e. DAPI for nuclei and CK18 for epithelial cells), and use the fluorochrome signature to differentiate individual antibodies while removing background to optimise signal-to-noise ratios. The intensity profiles generate features, including mean, maximum and standard deviation for each labelled antibody. Relationships of individual markers with their activated forms (e.g. pKDR:KDR, pEGFR:EGFR) and the intensity of a specific marker in cells that express another marker (e.g. phosphorylated mTOR in pERK-positive epithelial cells) are generated through the script feature analysis software. The scripts generated 84 features for entry in the models.

2.7. *Statistical analysis*

Time to death was defined as the time from initiation of gefitinib treatment to date of death or date of the last follow-up, and was reported in weeks. Patients with no death recorded were censored at the date of the last follow-up.

We applied support vector regression for censored data with feature reduction (SVRc-FR)[10–12] on clinical variables and features generated by M-Plex™, histologic morphometry and EGFR immunohistochemistry. SVRc,[10–12] an adaptation of SVR for accommodating censored data, uses a modified loss/penalty function that allows processing of right-censored and non-censored data. SVRc-FR uses an initial filtering step to remove features not univariately correlated with the outcome of interest, based on the concordance index (CI), which is the probability of predicting the correct order of events for two randomly chosen patients, where both died, or one died before the last follow-up of the other. The CI ranges from 0 to 1, with 0.5 indicating a random association. CIs further from 0.5 thus indicate stronger associations with outcome. In SVRc-FR, only features with CI <0.4 or >0.6 are retained.[14,15]

The SVRc-FR algorithm initially builds a model incorporating all features. In each succeeding model, the algorithm eliminates the feature with the lowest contribution (defined as the feature weight in the model multiplied by the square root of the standard deviation of the feature values from all patients). The output model is the one with the best CI from all models built.

For cut-point analysis, all model scores were examined as candidates for the optimal cut-point, defined by the maximum chi-square; the p-value was adjusted to account for inflation in type I error.

Multivariable Cox models were constructed using a stepwise approach. All features with p-value $\leqslant 0.15$ were entered into the model. To stay in the model, a feature needed p-value $\leqslant 0.05$.

3. Results

Tissue samples from 109 of the 284 patients (38%) had sufficient tumour (>50%) for further analyses. Patient characteristics are shown in Table 2.

3.1. EGFR mutations

EGFR mutation analysis based on the known mutations in exons 19–21[5,6,8] was performed on the 87 patients who had clinical outcome data and sufficient material for DNA analysis. Their median overall survival was 24 weeks, and the 1-year overall survival was 26%. Four patients (5%) had an EGFR tyrosine kinase domain mutation in exon 19, 20 or 21. Two of these were in-frame deletions (delL747-S752insV and delL747-P753insS), and two were point mutations (T790M or L858R). All the four patients with EGFR mutation were female, and had been diagnosed with adenocarcinoma. Two of these patients had achieved partial response and two progressed (Table 3).

Because of the low frequency of EGFR mutations, mutation status was not used as a variable in subsequent model development.

3.2. EGFR immunohistochemistry

EGFR was analysed by immunohistochemistry in regions of tumour in the 61 patient samples for which tumour represented >50% of the sample area. The tumour staining index varied greatly among samples. Fourteen samples (23%) exhibited a staining index $\geqslant 200$ suggestive of increased expression, while 20 (30%) had a staining index of 0. The tumour staining index was the only immunohistochemistry variable included in the predictive model.

3.3. Image analysis

Selected digitised images from 109 H&E-stained patient samples were processed with imaging software. The software segments and classifies individual tissue/cellular elements, segregating epithelial nuclei, epithelial cytoplasm, stroma and alveolar lumens. Elements are classified using spectral 'colour' characteristics, shape and spatial relationships between tissue objects. Lumen, for example, is classified from a pattern of white space surrounded by alveolar 'tumour' epithelial cells. An example of a digitised H&E image before and after segmentation is shown in Fig. 1. Thirty-nine imaging features (including properties of epithelial nuclei, cytoplasm, stroma and lumen) were generated and entered into the predictive models.

Table 2 – Characteristics of patients in the final predictive model compared with the full cohort.

Characteristic	51 Patients in model: N (%)	Full cohort of 284: N (%)
Performance status		
0	2 (3.9)	13 (4.58)
1	39 (76.5)	203 (71.48)
2	10 (19.6)	68 (23.94)
Gender		
Female	22 (43.1)	126 (44.37)
Male	29 (56.9)	158 (55.63)
Histology		
Adenocarcinoma	31 (60.8)	138 (48.59)
Bronchoalveolar	1 (2.0)	5 (1.76)
Large cell	5 (9.8)	36 (12.68)
Mixed	2 (3.9)	20 (7.04)
NSCL	5 (9.8)	30 (10.56)
Squamous	7 (13.7)	55 (19.37)
Smoking history		
No	8 (15.7)	45 (15.85)
Yes	43 (84.3)	239 (84.15)
Chemotherapy regimens		
0	1 (2.0)	19 (6.69)
1	19 (37.3)	106 (37.32)
2–3	25 (49.0)	135 (47.54)
4–6	6 (11.8)	24 (8.45)
Age		
Mean ± SD	60.8 ± 12.83	63.02 ± 11.29
Median	62.0	64.0
Range	24.0–82.0	24.0–86.0
Survival		
Deaths	50 (98.0)	268 (94.37)
Median survival, weeks	25.0	27.0

Table 3 – Outcomes of patients with EGFR mutations.

Patient number	Exon	Mutation	Objective response	Time to death, weeks
46	19	del L747-S752insV	Partial response	65
127B	19	del L747-P753insS	Partial response	92
69	21	L858R	Progression	22
196	20	T790M	Progression	4

3.4. *Quantitative M-Plex™ immunofluorescence*

All 15 antibodies exhibited the expected cellular localisation and distribution on control tissue samples (data not shown). Tumour specimens from 59 patients were assessed. Representative regions of interest for each antibody were selected based on quantity and quality of tumour within the sample, avoiding regions of necrosis and cellular debris. At least three fields were acquired per patient sample in each multiplex analysis, and all images were processed using the immunofluorescence software to generate 84 quantitative features, which reflected protein signal intensity and area within tumour epithelial cells.

The antigens under evaluation represented specific pathways involved in cell cycle regulation, apoptosis and angiogenesis. Of significance, cyclin D1 was present within nuclei of tumour epithelial cells (Fig. 2A and E), and was absent in the selected specimens of bronchoalveolar carcinoma histology (Fig 2B). Activated caspase-3 (Fig. 2C and F) was present focally in tumour epithelial cells and infiltrating lymphocytes, while pKDR (Fig. 2D and G) was present in both tumour epithelial cells and stromal endothelial cells. VEGF co-localised with pKDR (data not shown), supporting an autocrine–paracrine mechanism within NSCLC. Finally, phosphorylated mTOR was localised to tumour cells in both cytoplasm and nuclei (Fig. 2H).

3.5. *Predictive models*

Models were based on data from the 51 patients for whom we obtained complete data (clinical, immunohistochemistry and immunofluorescence). Characteristics of these patients were similar to those of the overall cohort (Table 2).

Using an integrative 'systems pathology' approach, we developed eight models of overall survival, based on clinical variables plus different combinations of the other three feature domains: EGFR immunohistochemistry, histologic morphometry and immunofluorescence. Because the single EGFR immunohistochemistry feature did not pass the CI filter for model inclusion, the four models incorporating the immunohistochemistry domain were identical to models without this domain. Table 4 shows the four unique models and the features selected, which are listed in order of their importance in the model as indicated by contribution. A positive contribution for a feature means that higher values of the feature predict a better outcome (longer survival time), and a negative contribution means that higher values predict a worse outcome.

The model incorporating clinical, immunofluorescence and histologic morphometry data had the best performance (CI, 0.74), and was selected as the final model. By comparison, the model incorporating only clinical data produced a CI of 0.62.

Model scores were analysed by a chi-squared statistic based on the log-rank test.[16] A cut-point of 39.5 most strongly separated patients in terms of their actual survival experience (chi-square, 21.39; adjusted $p = 0.0002$). Scores above 39.5 had a hazard ratio of 5.26 (95% confidence interval: 2.60–10.62) for risk of death over the study period. Kaplan–Meier curves for patients above and below the cut-point are shown in Fig. 3.

The predictive value of individual features was further tested by multivariable Cox analysis. Performance status

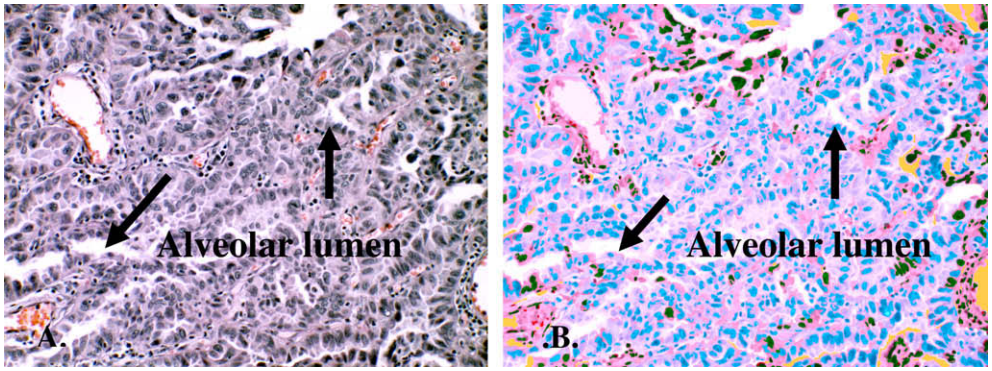

Fig. 1 – Standard digitised H&E image of primary NSCLC (adenocarcinoma; bronchoalveolar type). (A) Representative region demonstrating alveolar lumen (arrows) and compact tumour epithelial cells lining alveolar spaces. (B) The same image after processing with image analysis software. Cellular components are classified with respect to compartment: epithelial cytoplasm (light purple), epithelial nuclei (blue), stroma (pink), stromal nuclei including endothelial cells (green), alveolar lumen (white space; arrows). Magnification, 200×. (For interpretation of the references to color in this figure legend, the reader is referred to the web version of this article.)

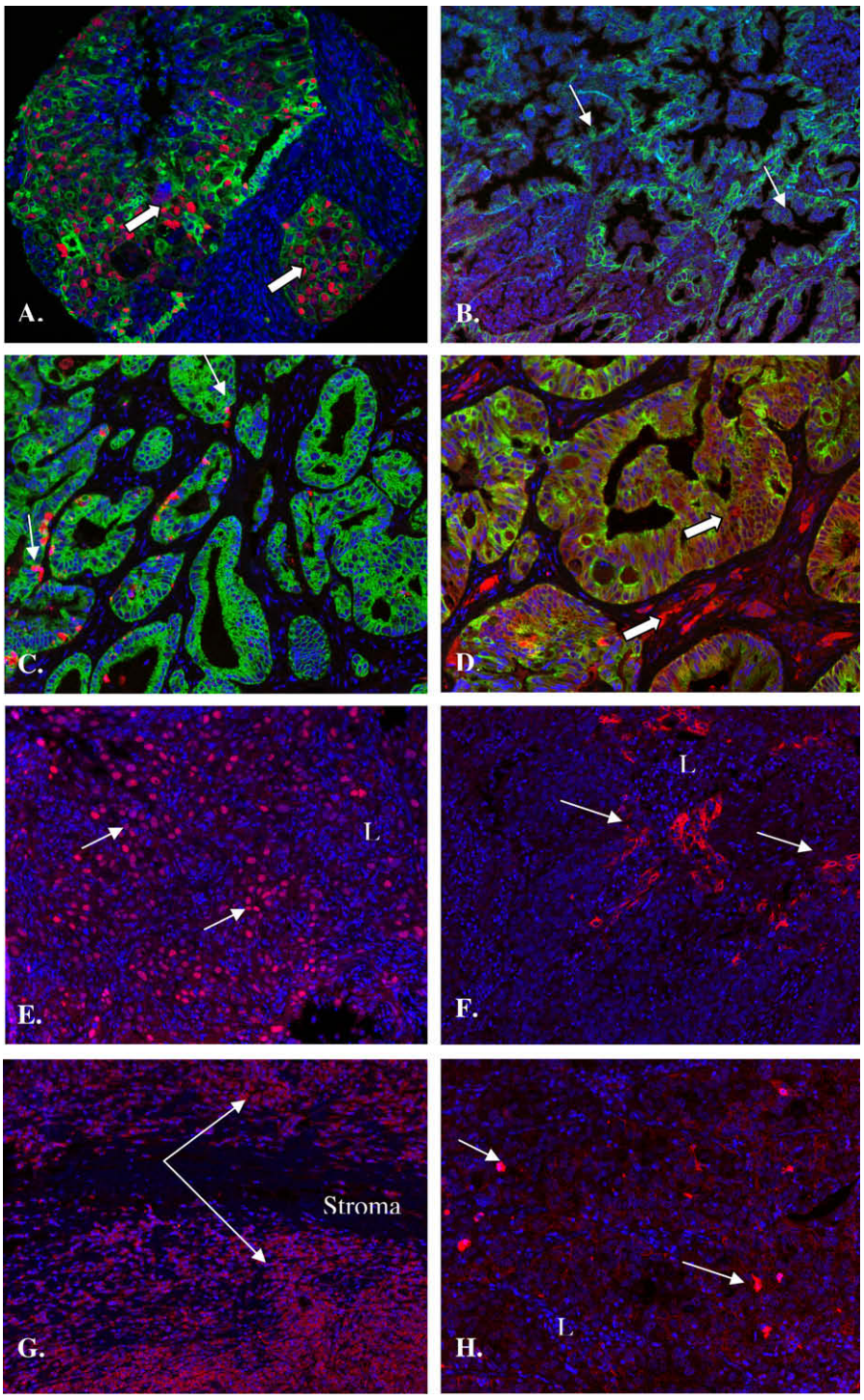

Fig. 2 – Representative examples of antibody:antigen distribution within NSCLC specimens. Composite images of Cyclin D1 (red; white arrows) in tumour epithelial nuclei of undifferentiated adenocarcinoma (A) and bronchoalveolar carcinoma (B); (CK18 epithelial cells – green; DAPI nuclei blue). Composite images of Caspase-3 activated (C) and phosphorylated KDR (D) (red; white arrows) focally in tumour epithelial cytoplasm and nuclei, respectively. Combined biomarker (red) plus DAPI (nuclei-blue) illustrates heterogeneity of antigen distribution within cellular compartments from different patient samples: cyclin D1 (E, white arrows, L = lymphocytes), Caspase-3 activated (F, white arrows, L = lymphocytes), phosphorylated KDR (G, white arrows) and phosphorylated mTOR (H, white arrows, L = lymphocytes). Magnification, 200×. (For interpretation of the references to color in this figure legend, the reader is referred to the web version of this article.)

was a significant predictor of survival across all models (hazard ratio (HR) in the four-domain model, 4.4; 95% confidence interval, 1.96–9.92). Cyclin D1, pKDR, caspase-3, VEGF and pERK were selected multiple times in various models,

Table 4 – SVRc-FR models.

Domains	CI of best model	Features chosen (in the order of importance)	Feature contribution
Clinical	0.62	Performance status	–4.766
Clinical + IF	0.73	Performance status	–4.766
		Caspase-3 mean intensity	–2.4688
		Cyclin D1 overall intensity	–2.2744
		pKDR variability	–2.1261
		Cyclin D1 mean intensity	–2.0558
Clinical + H&E	0.68	Performance status	–4.766
		Relative area of lumen	2.5081
Clinical + IF + H&E	0.74	Performance status	–4.766
		Caspase-3 mean intensity	–2.5079
		Cyclin D1 overall intensity	–2.3232
		pKDR variability	–2.1663
		Cyclin D1 mean intensity	–2.0788
		Relative area of lumen	1.9107

IF, immunofluorescence.

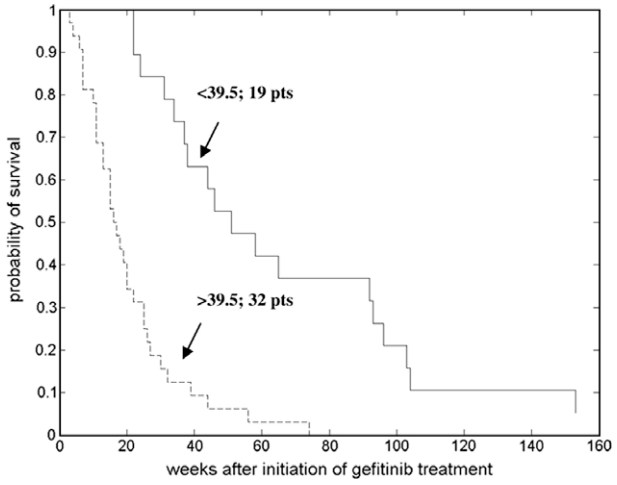

Fig. 3 – Survival curves for the 51 patients in the model, separated into groups with model score above or below the cut-point of 39.5.

although in different derived features reflecting different attributes of the marker.

4. Discussion

There is a general consensus on the importance of identifying patients with NSCLC who are likely to derive clinical benefit from treatment with gefitinib. We investigated gefitnib response in an advanced disease NSCLC cohort, and identified a constellation of clinical and tumour-specific features that were predictive for overall survival. By integrating quantitative biomarker characteristics and histologic morphometry with clinical data, we have been able to increase the accuracy or concordance index (CI) of prediction from 62% (clinical features alone) to 74% (all domains). This 12% increase represents a substantial improvement in predictive accuracy given that fairly modest improvements in the CI of predictive models, as described for prostate cancer outcome, e.g. from 0.77 to 0.79, have been reported as clinically significant.[17]

The present study included only patients treated with gefitinib; therefore, we cannot distinguish whether the features identified are associated with longer survival on gefitinib alone (predictive factors), or with longer survival regardless of treatment (prognostic factors). Prospective randomised controlled studies are required to evaluate this further.

In the current EAP cohort, we identified EGFR mutations in 4 of 87 patients which is comparable to what has been reported for other Western groups.[18] One patient with a reduced survival time (4 weeks) had a T790M mutation in their primary tumour specimen, which had been previously associated with drug resistance.[19] Although the overall frequency of EGFR mutation was too low for inclusion in the predictive models, the original published results on 124 patients from this cohort had identified that 45% had no evidence of progression at first re-evaluation and 29% reported improvement in lung cancer-related symptoms while receiving gefitinib.[20] The evidence of a potential positive clinical effect with a low mutation rate would suggest that additional factors may be more reflective of tumour response in addition to EGFR mutation status.

Of the six clinical variables analysed, only performance status was selected in the multivariate model. This agrees with an earlier study which demonstrated that good performance status was associated with a longer survival time.[21] By comparison, the clinical tumour histology, in particular bronchoalveolar variant, which has been associated with good clinical outcome in prior studies,[5,22] was not selected in any of the predictive models. However, the single morphometric feature representing the amount of alveolar space present within the tumour sample was selected, and we hypothesise that this feature represents a surrogate for the bronchoalveolar tumour histology. By increasing the amount of alveolar space, the model is registering the amount of bronchoalveolar tumour present within the specimen, and this is associated with good outcome.[19]

The molecular mechanisms underlying gefitinib sensitivity in NSCLC remain incompletely understood. In addition to EGFR mutation status and EGFR gene copy number, other molecular variables have been investigated including the immunohisto-

chemical expression of both EGFR and pEGFR, as well as downstream signalling molecules such as PI3K, pAKT and pERK1/2. Unfortunately, there is a disagreement and scant scientific evidence on the role, if any, that these factors play in gefitinib sensitivity, particularly for overall survival. Even EGFR immunohistochemistry has yielded conflicting results on its association with gefitinib response.[4,23,24]

In the current analysis, several quantitative immunofluorescent markers were associated with overall survival. Of significance, two cyclin D1 features were selected by the final model, with increased amounts associated with shortened survival time. Although published studies on the prognostic role of cyclin D1 are conflicting, two efforts support the conclusion that over-expression is associated with shorter survival time.[25,26] The observed discordance between studies may result from technical challenges related to performing and interpreting immunohistochemistry on formalin-fixed lung samples.

Another biomarker selected by the final model, caspase-3, has also been the subject of conflicting reports linking over-expression with survival.[27,28] We found that increasing levels of caspase-3 were associated with a reduced survival time, and we postulate that this tumour profile may reflect accelerated cell turnover driven by a dysregulated apoptotic mechanism. For the final selected marker, pKDR, there is limited tissue data and only on the non-phosphorylated form (i.e. VEGFR2), whereby increased expression was associated with a poor prognosis.[29] In our Cox models, increased levels of VEGF were associated with reduced survival; consistent with the earlier studies examining VEGF in conjunction with micro-vessel density and tumour invasion.[30] The repeated selection of cyclin D1, caspase-3 activated, pKDR and VEGF in our various sub-models emphasises the importance of cell cycle regulation, apoptosis and angiogenesis in the growth and progression of NSCLC.

In conclusion, we have developed an early-stage system-based model that predicts overall survival in advanced NSCLC patients treated with gefitinib. Further validation on an external cohort in a randomised setting would be necessary for confirmation.

Conflict of interest statement

Michael Donovan is a paid consultant for Aureon Laboratories; Valentina Zubek-Bayer and Mikhail Teverovskiy are full time employees of Aureon Laboratories; Both Carlos Cordon-Cardo and Jose Costa are scientific founders and current board members of Aureon Laboratories; Angeliki Kotsianti and David Verbel were former employees of Aureon Laboratories, and are current stock holders of Aureon Laboratories.

Dinah Parums is a former employee of AstraZeneca.

Acknowledgements

We thank Drs. Judy Ochs and Alan Barge for clinical input, and Drs. Brian Holloway, Claire Watkins, Rose McCormack and Georgina Speake from the Iressa Science team at AstraZeneca for scientific and statistical input and helpful discussions. We also thank all support personnel at Aureon, including Faysal Elkhettabi, Olivier Saidi, Faisal Khan, Marina Sapir, Peter Angione, Mark Clayton, Stefan Hamann, Henry Pang, Yevgen Vengrenyuk, and Nicole Roberts. Special thanks to Janet Novak for insightful commentary on the manuscript. This work was supported in part by AstraZeneca and Aureon Laboratories.

REFERENCES

1. Giaccone G, Herbst RS, Manegold C, et al. Gefitinib in combination with gemcitabine and cisplatin in advanced non-small-cell lung cancer: a phase III trial–INTACT 1. *J Clin Oncol* 2004;**22**:777–84.
2. Herbst RS, Giaccone G, Schiller JH, et al. Gefitinib in combination with paclitaxel and carboplatin in advanced non-small-cell lung cancer: a phase III trial–INTACT 2. *J Clin Oncol* 2004;**22**:785–94.
3. Thatcher N, Chang A, Parikh P, et al. Gefitinib plus best supportive care in previously treated patients with refractory advanced non-small-cell lung cancer: results from a randomised, placebo-controlled, multicentre study (Iressa Survival Evaluation in Lung Cancer). *Lancet* 2005;**366**:1527–37.
4. Dudek AZ, Kmak KL, Koopmeiners J, Keshtgarpour M. Skin rash and bronchoalveolar histology correlates with clinical benefit in patients treated with gefitinib as a therapy for previously treated advanced or metastatic non-small cell lung cancer. *Lung Cancer* 2006;**51**:89–96.
5. Lynch TJ, Bell DW, Sordella R, et al. Activating mutations in the epidermal growth factor receptor underlying responsiveness of non-small-cell lung cancer to gefitinib. *New Engl J Med* 2004;**350**:2129–39.
6. Paez JG, Janne PA, Lee JC, et al. EGFR mutations in lung cancer: correlation with clinical response to gefitinib therapy. *Science* 2004;**304**:1497–500.
7. Cappuzzo F, Hirsch FR, Rossi E, et al. Epidermal growth factor receptor gene and protein and gefitinib sensitivity in non-small-cell lung cancer. *J Natl Cancer Inst* 2005;**97**:643–55.
8. Sequist LV, Martins RG, Spigel D, et al. First-line gefitinib in patients with advanced non-small-cell lung cancer harboring somatic EGFR mutations. *J Clin Oncol* 2008;**26**:2442–9.
9. Kim ES, Hirsh V, Mok T. Gefitinib versus docetaxel in previously treated non-small cell lung cancer (INTEREST): a randomized phase III trial. *Lancet* 2008;**372**:1809–18.
10. Cordon-Cardo C, Kotsianti A, Verbel DA, et al. Improved prediction of prostate cancer recurrence through systems pathology. *J Clin Invest* 2007;**117**:1876–83.
11. Muss HB, Bunn JY, Crocker A, et al. Cyclin D-1, interleukin-6, HER-2/neu, transforming growth factor receptor-II and prediction of relapse in women with early stage, hormone receptor-positive breast cancer treated with tamoxifen. *Breast J* 2007;**13**:337–45.
12. Donovan MJ, Hamann S, Clayton M, et al. Systems pathology approach for the prediction of prostate cancer progression after radical prostatectomy. *J Clin Oncol* 2008;**26**:3923–9.
13. Saidi O, Cordon-Cardo C, Costa J. Technology insight: will systems pathology replace the pathologist? *Nat Clin Pract Urol* 2007;**4**:39–45.
14. Yan L, Verbel D, Saidi O. Predicting prostate cancer recurrence via maximizing the concordance index. In: Kohavi R, Gehrke J, DuMouchel W, Ghosh J, editors. *Proceedings of the tenth ACM SIGKDD international conference on knowledge discovery and data mining*. ACM Press; 2004. p. 479–85.
15. Zubek V, Verbel D, Saidi O. Censored time trees for predicting time to PSA recurrence. In: *Proceedings of the fourth international conference on machine learning and applications (ICMLA*

2005). Washington, DC: IEEE Computer Society. p. 221–6.
16. Mazumdar M, Glassman JR. Categorizing a prognostic variable: review of methods, code for easy implementation and applications to decision-making about cancer treatments. *Stat Med* 2000;**19**:113–32.
17. Stephenson AJ, Scardino PT, Eastham JA, et al. Preoperative nomogram predicting the 10-year probability of prostate cancer recurrence after radical prostatectomy. *J Natl Cancer Inst* 2006;**98**:715–7.
18. Jeon YK, Sung SW, Chung JH, et al. Clinicopathologic features and prognostic implications of epidermal growth factor receptor (EGFR) gene copy number and protein expression in non-small cell lung cancer. *Lung Cancer* 2006;**54**:387–98.
19. Bell DW, Gore I, Okimoto RA, et al. Inherited susceptibility to lung cancer may be associated with the T790M drug resistance mutation in EGFR. *Nat Genet* 2005;**37**:1315–6.
20. Hainsworth JD, Mainwaring MG, Thomas M, et al. Gefitinib in the treatment of advanced, refractory non-small-cell lung cancer: results in 124 patients. *Clin Lung Cancer* 2003;**4**:347–55.
21. Su WP, Yang CH, Yu CJ, Shih JY, Hsu C, Yang PC. Gefitinib treatment for non-small cell lung cancer – a study including patients with poor performance status. *J Formos Med Assoc* 2005;**104**:557–62.
22. Erman M, Grunenwald D, Penault-Llorca F, et al. Epidermal growth factor receptor, HER-2/neu and related pathways in lung adenocarcinomas with bronchioloalveolar features. *Lung Cancer* 2005;**47**:315–23.
23. Bailey L, Janas M, Schmidt K, et al. Evaluation of epidermal growth factor receptor (EGFR) as a predictive marker in patients with non-small-cell lung cancer (NSCLC) receiving first-line gefitinib combined with platinum-based chemotherapy. *J Clin Oncol* 2004;**22**:7013 [abstr.].
24. Bailey L, Kris M, Wolf M, et al. Tumor EGFR membrane staining is not clinically relevant for predicting response in patients receiving gifitinib (Iressa, ZD 1839) monotherapy for pretreated advanced non-small-cell lung cancer: IDEAL 1 and 2. *Proc Am Assoc Cancer Res* 2003;**44**:1362. abstr..
25. Jin M, Inoue S, Umemura T, et al. Cyclin D1, p16 and retinoblastoma gene product expression as a predictor for prognosis in non-small cell lung cancer at stages I and II. *Lung Cancer* 2001;**34**:207–18.
26. Keum JS, Kong G, Yang SC, et al. Cyclin D1 overexpression is an indicator of poor prognosis in resectable non-small cell lung cancer. *Brit J Cancer* 1999;**81**:127–32.
27. Koomagi R, Volm M. Relationship between the expression of caspase-3 and the clinical outcome of patients with non-small cell lung cancer. *Anticancer Res* 2000;**20**:493–6.
28. Takata T, Tanaka F, Yamada T, et al. Clinical significance of caspase-3 expression in pathologic-stage I, nonsmall-cell lung cancer. *Int J Cancer* 2001;**96**(Suppl.):54–60.
29. Seto T, Higashiyama M, Funai H, et al. Prognostic value of expression of vascular endothelial growth factor and its flt-1 and KDR receptors in stage 1 non-small-cell lung cancer. *Lung Cancer* 2006;**53**:91–6.
30. Mineo TC, Ambrogi V, Baldi A, et al. Prognostic impact of VEGF, CD31, CD34, and CD105 expression and tumour vessel invasion after radical surgery for IB-IIA non-small cell lung cancer. *J Clin Pathol* 2004;**57**:591–7.